

A comparative study to elucidate the inhibitory mechanism of a 6-mer fragment of amyloid-beta 42 peptide as a potential therapeutic in Alzheimer's disease: insights from molecular dynamics simulations

Mary Dutta and Venkata Satish Kumar Mattaparthi*

Department of Molecular Biology and Biotechnology, Tezpur University, Sonitpur 784 028, India

Alzheimer's disease is a neurodegenerative and incurable disease that is associated with the amyloid beta (A β) aggregation. We have carried out comparative molecular dynamics simulations of a 6-mer peptide and its analogues to elucidate the inhibitory mechanism on A β aggregation. The top analogue screened after refinement via docking exhibited significant inhibitory activities on both A β ₁₇₋₄₂ fibril as well as A β ₁₋₄₂ monomer, leading to disassembly of β -strands of A β ₁₋₄₂ peptide and fibril by interacting with C-terminal residues via hydrogen bonds and hydrophobic contacts. Binding of the analogue to the C-terminal region proves to be significant.

Keywords: Alzheimer's disease, aggregation, docking, hydrophobic interaction, inhibitor peptide.

AMYLOIDOSIS stems from the accumulation of insoluble protein fibrils in an abnormal form¹. Amyloids, the aggregates formed by self-association of such insoluble protein fibrils, are associated with Alzheimer's disease (AD), which is one of the most common forms of dementia². Transgenic modelling studies have demonstrated the key role of amyloid beta (A β) peptides in the etiology of AD³. Isoforms of A β are generated by sequential cleavage of amyloid precursor protein (APP) by β - and γ -secretases enzymes⁴. A β ₁₋₄₂ peptide which is normally more toxic, exists as an unordered random coil, later exhibits a transition towards cross- β -sheet pattern in abnormal conditions⁵, and finally aggregates to form the matured fibrils. Amyloid fibrils form cross- β -sheet structures by the association of β -strands, where the individual β -strands are arranged in a parallel, in-register form⁶, wherein formation of disulphide bonds plays a critical role in initiating the fibrillation process⁷.

Different strategies have been developed to inhibit the formation of amyloid fibrils^{8,9}. Studies report that few molecules can even disintegrate preformed amyloid fibrils¹⁰. Inhibitors may inhibit amyloid formation by

binding and stabilizing the native folded state of a protein or by binding to aggregation-prone regions of amyloidogenic peptides and thereby prohibit self-assembly⁸. Although a number of compounds targeting β - or γ -secretases have made up to clinical trials, many such compounds have failed lately. Likewise, most immunotherapies that have shown progress in the reduction of A β ₁₋₄₂ peptide load have caused adverse events that are yet to be resolved. The metal chelators PBT1 and PBT2 developed to disrupt the interactions between A β ₁₋₄₂ peptide and metals failed during the clinical trials¹¹. Likewise, the approaches based on small molecules such as curcumin¹², RS0406¹³ and some polyphenols¹⁴ have not yielded therapeutically important molecules.

Ever since A β ₁₋₄₂ peptide is known to bind to itself, it can be used as a lead in generating novel fragments that can be modified as inhibitors for the parent peptide. In recent studies, many modified peptides derived from the central hydrophobic region of the A β ₁₋₄₂ peptide sequence have been designed as inhibitors for its aggregation¹⁵⁻²⁰. One of the inhibitors which has been modified based on A β ₁₇₋₂₁ fragment has completed phase II clinical trials in humans²¹. Similarly, it has been reported that a series of A β ₁₋₄₂ C-terminal fragments act as the most effective inhibitors of A β ₁₋₄₂ peptide-induced toxicity²². Another study has successfully designed N-methylated hexapeptides based on fragment A β ₃₂₋₃₇, which proved to be efficient inhibitors of A β ₁₋₄₂ aggregation²³. The molecules that possess high binding affinity for the C-terminus of A β ₁₋₄₂ peptide may disrupt the self-aggregation of A β ₁₋₄₂.

It is known that hydrophobic interactions play an important role in protein aggregation. It has also been suggested that the hydrophobic C-terminus of A β ₁₋₄₂ peptide can control its self-aggregation. Therefore, the designing of inhibitors has shifted to the central hydrophobic sequence of A β ₁₋₄₂ peptide^{24,25}. Inhibitors based on C-terminus fragments can easily bind to the parent peptide, and thus may prohibit amyloid formation. Bansal *et al.*²⁶ have reported a number of peptide-based inhibitors that displayed significant A β aggregation inhibitory activity

*For correspondence. (e-mail: venkata@tezu.ernet.in)

on both the isoforms. They have taken the 6-mer A β ₃₂₋₃₇ fragment as lead peptide and synthesized 42 new peptides by replacing all six amino acids by amino acids of both natural and unnatural origin which are isosterically analogous. From the methyl thiazol tetrazolium (MTT)-based cell viability assay, lead peptide was found to completely protect cells from A β ₁₋₄₂ and A β ₁₋₄₀ peptide-induced toxicity and the other ten analogous peptides were found to be moderately active on A β ₁₋₄₀-induced toxicity. Additionally CD spectroscopy and morphological examination by transmission electron microscopy confirmed the results.

Bansal *et al.*²⁶ found the reference peptide to completely protect cells from A β ₁₋₄₂ and A β ₁₋₄₀ peptide-induced toxicity and the reported analogues to be moderately active on A β ₁₋₄₀-induced toxicity. However, they have not studied the effect of the analogues on A β ₁₋₄₂-induced toxicity. In the present study, we used lead peptide and the reported analogues of natural origin to study the molecular recognition and inhibitory mechanism using MD simulations.

All the 7 analogues of natural origin were assessed via docking to check their binding affinities to A β ₁₋₄₂ monomer and A β ₁₇₋₄₂ fibril relative to the original peptide. We found analogue 6 (IGLMVV) to have higher ACE and the surface area relative to reference peptide. Analogue 6 was therefore used to study its inhibitory effect on the A β ₁₇₋₄₂ fibrils. Also, the top scoring analogue 6 was assessed by performing unbinding MD simulations with the A β ₁₋₄₂ monomer in explicit solvent subsequently generating their potential of mean force (PMF)²⁷ using umbrella sampling (US) simulations²⁸. The analogue 6-A β ₁₋₄₂ monomer complex was first equilibrated in a box of water. Analogue 6 was then pulled apart at a constant rate, the forces monitored, and the free energy change calculated as a function of separation. The detailed energetics of the complex formation and the conformational changes undergone by the A β ₁₋₄₂ monomer were monitored. The revelation of binding regions of the A β ₁₋₄₂ monomer with the analogue 6 will help in designing more effective inhibitors for A β ₁₋₄₂ aggregation.

Materials and methods

Construction of input files for docking

Computational model of initial A β ₁₋₄₂ peptide monomer: The initial A β ₁₋₄₂ peptide monomer (PDB ID: 1IYT)²⁹ was retrieved from the RCSB Protein Data Bank³⁰. Counter ions (3 Na⁺) were added to make the net charge of the system zero. TIP3PBOX³¹ water model with 10 Å in all directions was used to solvate the system. Total number of particles in the system was 15885. Two minimization cycles were performed on the A β ₁₋₄₂ peptide monomer. The first cycle was performed under T, V, N conditions keeping the monomer fixed in order to relax

the water. The subsequent minimization was performed with no constraints on the monomer. After the energy minimization, we gradually heated up the minimized structure from 0 K to 300 K over 20 ps in a total of 6 stages (0 to 50 K, 50 to 100 K, 100 to 150 K, 150 to 200 K, 200 to 250 K and 250 to 300 K). Heating in stages reduces the chances of the system blowing up by allowing it to equilibrate at each temperature. This is essential to avoid problems with hot solvent cold solute. The system was then equilibrated at 300 K for 100 ps which is sufficient for equilibration. Finally, 80 ns of NPT (number, pressure, temperature) MD simulations was carried out. The conformer with β -strands generated from trajectory analysis was used for docking.

MD simulations at 300 K and 1 bar pressure were performed in explicit solvent using AMBER 12 (ref. 32) package with the most recent force field ff99SBildn (ref. 33). Periodic boundary conditions were applied. Berendsen thermostat was used to control the temperature and pressure of the system³⁴. Shake algorithm was used to constrain all bonds and the time step of the simulation was 2 fs (ref. 35). Non-bonded and electrostatic forces were evaluated at each time step. Electrostatics was computed using Particle Mesh Ewald (PME) method³⁶.

Computational model of initial reference peptide and the analogues: The initial reference peptide (IGLMVG) structure was extracted from the A β ₁₋₄₂ peptide (PDB ID: 1IYT)²⁹ using pymol³⁶. The reported seven analogues of natural origin were constructed from the initial reference peptide using Swiss-PDB Viewer³⁷. TIP3PBOX³¹ water model with 10 Å in all directions was used to solvate the system with reference peptide and analogues individually. A total of 3556 number of water particles were added to each system. Further minimization and equilibration was carried out as described in previously. The conformers of the reference peptide and the seven analogues representing the most populated clusters after equilibration were used for docking.

Computational model of A β ₁₇₋₄₂ fibril structure: The 2BEG³⁸ fibril structure was retrieved from the RCSB Protein Data Bank³⁰. Counter ions (5 Na⁺) were added to make the net charge of the system zero. TIP3PBOX³¹ water model with 10 Å in all directions was used to solvate the initial 2-BEG fibril structure. A total of 44,465 water particles were added. Further minimization and equilibration was carried out as described previously. The conformer representing the most populated cluster after equilibration was used for docking.

Docking of A β ₁₋₄₂ peptide, A β ₁₇₋₄₂ fibril and 6-mer peptide

The reference peptide (IGLMVG) and the analogues were first assessed by docking in PatchDock server⁴⁰ with

$A\beta_{1-42}$ monomer and $A\beta_{1-42}$ fibril respectively. This server applies the concept of geometric-based docking algorithm to select the optimum candidate with the RMSD clustering to remove the redundant models. Each model was given a score which implies docking transformation of one of the monomers which optimally fits with the other monomer inducing both wide interface areas and small amounts of steric clashes. In the present study, a default RMSD of 4 Å was considered. The docking scores of the reference peptide and the analogues with $A\beta_{1-42}$ monomer and $A\beta_{17-42}$ fibril were calculated. Analogue 6 that resulted in a higher docking score with maximum atomic contact energy and contact area when compared to the reference peptide was accepted.

The selected $A\beta_{1-42}$ /analogue 6 complex and the $A\beta_{1-42}$ /reference complex was solvated in TIP3P water model with a minimum distance of 10 Å to the border, and then subjected to a two-step restrained minimization, followed by heating as described previously. Within the box, the total number of particles in the system was 16796. The individual complexes were then equilibrated for 100 ps. As our initial complex structures had attained equilibration, we ran production MD simulations for 10 ns. The conformer with the most populated cluster from the last trajectory was used for the PMF study.

Potential of mean force

Umbrella sampling simulations with the Weighted Histogram Analysis Method (WHAM)⁴¹ was performed in which the centre of mass of the backbone atoms of receptor peptide $A\beta_{1-42}$ and analogue were attached via harmonic restraint of 2 kcal/mol/Å². The analogue 6 was then pulled with a constant velocity along the reaction coordinate (RC), which is defined as the distance between the entire C- α atom of the amino acids of receptor peptide $A\beta_{1-42}$ and the analogue 6. For each independent simulation, the complex was allowed to sample only within that window. PMF was calculated by combining the data from each window which was achieved by applying a harmonic restraint to the RC. In each window, we

have carried out 5 ns of simulation. To remove the non-equilibrium effects that may contaminate the PMF, the first 3 ns in each window were treated as an equilibrium phase, and as such were ignored for post-processing. The restart file of the previous step was used as the input file for the configuration in both increasing and decreasing cases. After an increment of 1 Å, windows were obtained. For each window 2 ns, NPT MD run was performed and for the next window the resulting equilibrated structure was used as the starting co-ordinate. After every MD run, the VMD package was used for the generated trajectories visualization⁴².

Results and discussion

Binding characteristics of the analogue

In the present study, we have carried out a comparative study to examine the inhibition mechanism of a 6-mer peptide. At the very beginning, we have evaluated the binding energy of the reference peptide and the reported analogues by docking. Analogue 6 (IGLMVV) was found to have the highest docking score. The docking score for the $A\beta_{1-42}$ monomer and $A\beta_{17-42}$ fibril is shown in Table 1. The binding conformations of analogue 6 with the $A\beta_{1-42}$ monomer and $A\beta_{17-42}$ fibril are shown in their bound form in Figure 1. Figure 1a shows the $A\beta_{1-42}$ monomer bound to the analogue 6. β -strand in the monomer is shown in green colour. Analogue 6 is shown in red color. In Figure 1b all the five strands are shown in different colours. Analogue 6 was selected to study the inhibitory mechanism against $A\beta_{1-42}$ aggregation. Analogue 6 was anchored to the amyloid fibril surface by its isoleucine at the N-terminal end. The hydrocarbon side chain of isoleucine fits into the hydrophobic glycine groove where it has hydrophobic interactions. Glycine and methionine of the analogue also form hydrophobic interactions with the methionine and closely located valine. Leucine was observed to form direct hydrogen bonds with valine. Their binding characteristics revealed a few key points. It can be concluded that hydrophobic interactions are the

Table 1. Docking result of the 6-mer peptides with $A\beta_{1-42}$ monomer and $A\beta_{17-42}$ fibril respectively

6-mer peptide	6-mer peptide sequence	6-mer peptide- $A\beta_{1-42}$ peptide monomer complex		6-mer peptide- $A\beta_{17-42}$ fibril complex	
		Area (Å ²)	ACE (kcal/mol)	Area (Å ²)	ACE (kcal/mol)
Reference peptide	Ile-Gly-Leu-Met-Val-Gly-NH2 (reference peptide)	498.50	-216.23	570.50	-286.81
Analogue 1	Ile-Val-Leu-Met-Val-Gly-NH2	548.20	-310.39	601.50	-342.46
Analogue 2	Ile-Gly-Phe-Met-Val-Gly-NH2	565.90	-277.33	581.70	-267.65
Analogue 3	Ile-Gly-Leu-Met-Pro-Gly-NH2	505.90	-230.51	592.40	-325.67
Analogue 4	Ile-Gly-Leu-Met-Phe-Gly-NH2	535.40	-83.36	563.00	-353.57
Analogue 5	Ile-Gly-Leu-Met-Val-Ile-NH2	540.30	-50.96	611.00	-352.96
Analogue 6	Ile-Gly-Leu-Met-Val-Val-NH2	587.10	-305.00	600.70	-410.23
Analogue 7	Val-Gly-Leu-Met-Val-Gly-NH2	550.90	-269.53	584.30	-378.35

primary factor that facilitates analogue binding to the amyloid fibril and the monomer. The secondary factor appears to be the hydrogen bonds.

Effect of the analogue on A β ₁₇₋₄₂ fibril

A β ₁₋₄₂ peptides that normally adopt α -helix and random coil conformations in aqueous solution undergo transition in their secondary structures to form intramolecular β -sheet structures under abnormal conditions and aggregates. By MD simulation, we studied the effect of analogue 6 on the conformational transition of A β ₁₇₋₄₂ fibril. Figure 2 shows the conformational dynamics of A β ₁₇₋₄₂ fibril in the presence of the analogue. From Figure 2, we can see the initial complex structure of the A β ₁₇₋₄₂ fibril with analogue 6 bound to it. After 60 ns time interval we notice secondary structural transitions in A β ₁₇₋₄₂ fibril. After 80 ns time interval, we notice disassembly of the β -strands in the fibrils in the presence of analogue 6. Thus in the presence of analogue 6, the intermolecular interactions that hold the strands together in the fibril are destabilized; as a result, the amyloid fibril undergoes disassembly. Analogue 6 may thus impart its inhibitory effect by destabilizing various interactions and affecting the β -strands in A β ₁₇₋₄₂ fibril. We also ensured the efficiency of analogue 6 as a potent inhibitor from the outcome of control simulation ([Supplementary Figure 1](#)).

Potential of mean force for unbinding the analogue

We have computed the free energy profile of the association of the reference peptide and analogue 6 to the A β ₁₋₄₂ monomer to elucidate their interaction. The interaction was thus studied using US simulations with distance as a function of time whereby the relative binding affinities of the analogue-A β ₁₋₄₂ monomer complex were determined. Figure 3 shows the result of the free energy profile. The initial reference peptide and analogue A β ₁₋₄₂ monomer complex was formed at an inter-chain distance of 11 Å. As we pulled out the reference peptide from the A β ₁₋₄₂ monomer, we observed a high free energy of ~ 7 kcal/mol.

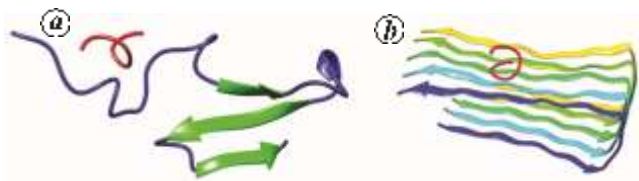


Figure 1. Structure of (a) the initial A β ₁₋₄₂ monomer/analogue 6 complex; (b) the initial A β ₁₇₋₄₂ fibril/analogue 6 complex with the highest atomic contact energy and surface area score obtained from Patch-Dock server.

The global minima structure was formed at an inter-chain distance of 11 Å. Thus it can be inferred that the reference peptide binds strongly with the A β ₁₋₄₂ monomer. In the case of analogue 6, as we pulled it out from the A β ₁₋₄₂ monomer, we observed a low van der Waals force of repulsion till a distance of ~ 16 Å. At a distance of ~ 16 Å the global minima structure was formed which exhibited minimum energy among all other conformations. After the global minima structure was formed the van der Waals force of attraction suddenly increased and dissociation energy was found to be quite high, around 4 kcal/mol.

Although the reference peptide was found to bind strongly to A β ₁₋₄₂ peptide when compared to analogue 6, the disappearance of β -strands in A β ₁₋₄₂ peptide is more pronounced in the presence of analogue 6 (can be seen from Figure 4) than in the presence of reference peptide as shown in [Supplementary Figure 2](#). In addition, we observed that the reference peptide binds to the N-terminal region of the A β ₁₋₄₂ peptide and analogue 6 binds to the C-terminal region of the A β ₁₋₄₂ peptide (Figure 4). As C-terminal region is crucial for A β ₁₋₄₂ peptide aggregation, binding of analogue 6 to the C-terminal region of A β ₁₋₄₂ peptide proves to be significant. Additionally, to study the binding characteristics of the reference peptide and analogue 6 with A β ₁₋₄₂ monomer, we isolated the global minima structures from the free energy profile and carried out analysis for the residue-residue contacts between the reference peptide and A β ₁₋₄₂ monomer as well as analogue 6 and A β ₁₋₄₂ monomer.

Interaction profile of the reference peptide and the analogue with A β ₁₋₄₂ peptide

The contacts between residues of A β ₁₋₄₂ peptide and reference peptide as well as the analogue were studied based on their shape and chemical complementarity using contact map analysis (CMA)⁴³. The analysis result displays atom-to-atom contacts for the pair of amino acid residues involved in the interaction in the form of a contact map. To study the residue-residue contacts in the present analysis, a contact area threshold above 8 Å² was set. These interactions can be attributed to non-specific hydrophobic contacts between C α atoms of the above residues. The propensity of interactions is primarily mediated by the presence of surface hydrophobic groups available for interaction. Figure 5 a and b displays the residues of A β ₁₋₄₂ monomer that interact with the reference peptide as well as analogue 6 respectively. From Figure 5 a we observe that most of the N-terminal residues of A β ₁₋₄₂ monomer interact with the reference peptide. On the contrary, from Figure 5 b we see that most of the residues involved in the interaction between A β ₁₋₄₂ monomer and analogue 6 belong to the C-terminal region and are hydrophobic in nature. Since it is known that the C-terminal

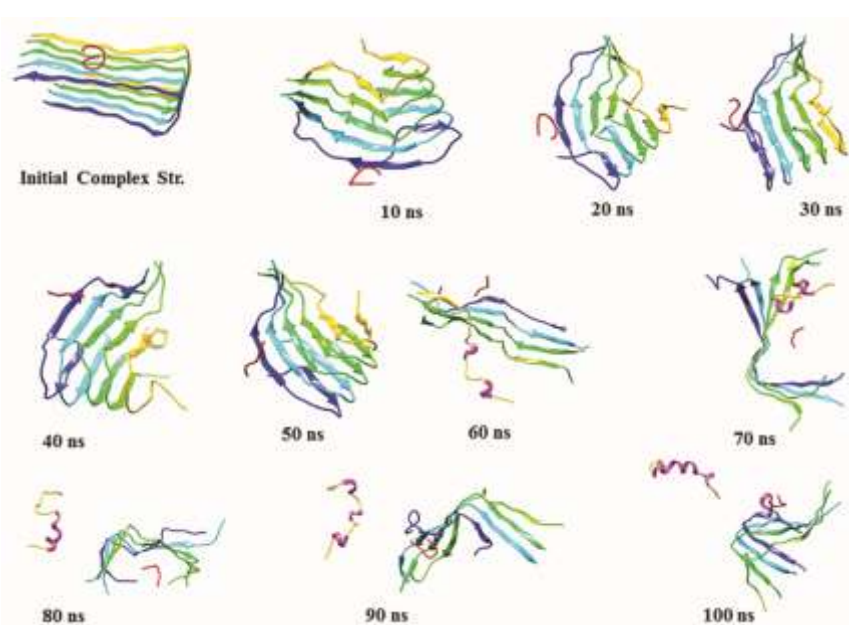


Figure 2. Conformational dynamics of $A\beta_{17-42}$ fibril in the presence of analogue 6 at different time courses of simulation at 300 K.

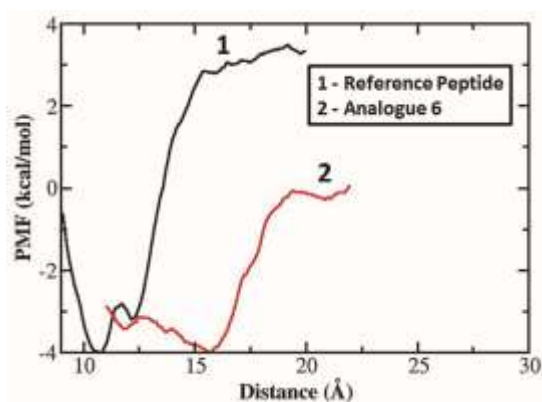


Figure 3. Potential of mean force of $A\beta_{1-42}$ monomer/reference peptide and $A\beta_{1-42}$ monomer/analogue 6 (in kcal/mol) as a function of the inter-chain distance (in Å) which is between the centre of mass of the C- α atom of two peptides.

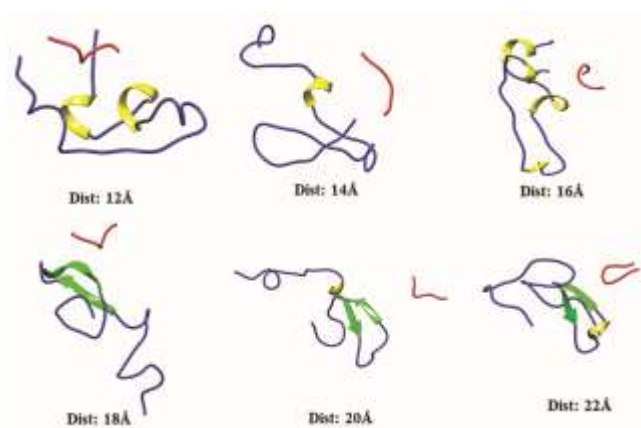


Figure 4. Snapshots of $A\beta_{1-42}$ monomer/analogue 6 complex at different inter-chain distances during the potential of mean force analysis at 300 K.

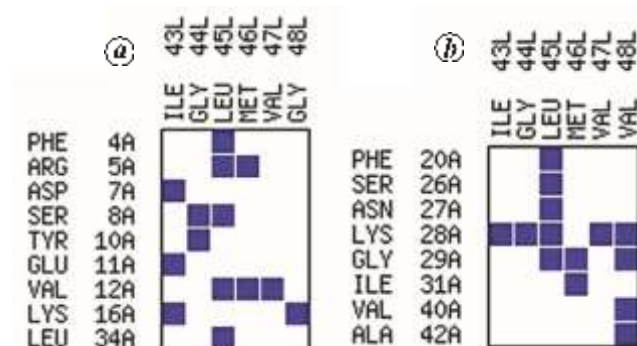


Figure 5. Contact map analysis showing residue-residue interactions in the global minima structure of: *a*, $A\beta_{1-42}$ monomer/reference peptide complex; *b*, $A\beta_{1-42}$ monomer/analogue 6 complex.

region plays an important role in the aggregation of $A\beta_{1-42}$ peptide, binding of the analogue 6 to the C-terminal region of $A\beta_{1-42}$ monomer seems crucial.

Furthermore, we also carried out the protein ligand interaction study using PDBSum server⁴⁴. The LigPlot results displaying $A\beta_{1-42}$ monomer-reference peptide interaction and $A\beta_{1-42}$ monomer-analogue 6 interactions are shown in Figure 6 *a* and *b* respectively. From Figure 6 *a* and *b* we observe hydrophobic interactions as well as hydrogen bonding to be the prime factors in governing the stability of the complex. Arg5, Tyr10, Glu11 and Lys16 of $A\beta_{1-42}$ monomer form hydrogen bonds with the reference peptide; His6, Ser8, Val12 and Leu34 form hydrophobic interactions (Figure 6 *a*). In the case of analogue 6, Ser26, Asn27, Ile31, Val40, Ile41 of $A\beta_{1-42}$ monomer form hydrophobic interactions (Figure 6 *b*). Lysine and glycine at positions 28 and 29 respectively form hydrogen

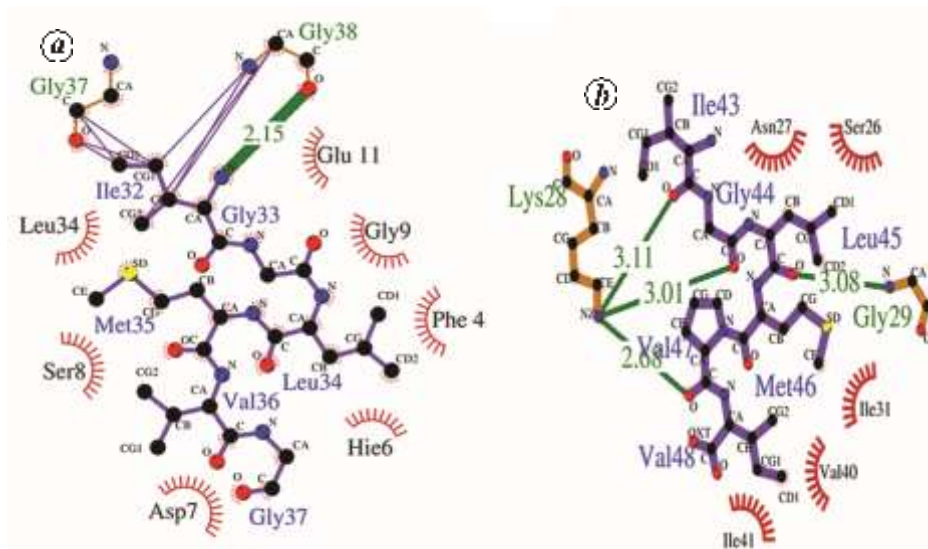


Figure 6. LigPlot analysis showing the interactions as predicted by the PDBSum server of the global minima structure of: *a*, A β ₁₋₄₂ monomer/reference peptide complex; *b*, A β ₁₋₄₂ monomer/analogue 6 complex.

bonds with the analogue. From the above results we see that the analogue binds to A β ₁₋₄₂ monomer mostly in the C-terminal end which is known as the aggregation prone area. We can expect this analogue to be a potent inhibitor of A β peptide aggregation.

Conclusion

We have carried out a comparative study using docking and MD simulations to elucidate the inhibitory mechanism of a 6-mer peptide on A β ₁₋₄₂ peptide aggregation. The results indicate one of the analogues (IGLMVV) to be a potent therapeutic candidate for A β ₁₋₄₂ peptide aggregation than the reference peptide. Our analogue shows promising results, provides insight into the inhibitor binding mechanism in detail, thus providing a direction for further drug designing analysis. The MD simulation of the analogue and fibril complex showed that the analogue binds to the fibril with a high affinity and thus imparts its inhibitory effect by dissociating the fibril to single strands. Also, it influences the secondary structural changes in the fibril as well as the monomer by decreasing the β -strand content. From the free energy analysis with the monomer, the affinity of the analogue can be confirmed to be strong. High dissociation energy specifies the strong affinity of the analogue to the peptide. Hydrophobic interaction plays an important role in the inhibitory mechanism of the analogue. Formation of strong hydrophobic interaction with the fibril as well as with the monomer leads to the dissociation of the fibril and loss of β -strands respectively. Although the free energy for the reference peptide is higher than the analogue, from the contact map analysis it was found that most residues of the A β ₁₋₄₂ monomer interacting with the ref-

erence peptide were from the N-terminal region. As C-terminal region is crucial for A β ₁₋₄₂ peptide–A β ₁₋₄₂ peptide interaction, binding of the analogue to the C-terminal region of A β ₁₋₄₂ peptide proves to be significant. In the light of the docking and the free energy results, we suggest the analogue to be a potent therapeutic agent.

Conflict of Interest: The authors declare no conflict of interest.

1. Tan, S. Y., Pepys, M. B. and Hawkins, P. N., Treatment of amyloidosis. *Am. J. Kidney Dis.*, 1995, **26**, 267–285.
2. Tycko, R., Progress towards a molecular-level structural understanding of amyloid fibrils. *Curr. Opin. Struct. Biol.*, 2004, **14**, 96–103.
3. Selkoe, D. J., Alzheimer's Disease: genotypes, phenotype, and treatments. *Science*, 1977, **275**, 630–631.
4. Haass, C. and Selkoe, D. J., Cellular processing of β -amyloid precursor protein and the genesis of amyloid β -peptide. *Cell*, 1993, **75**, 1039–1042.
5. Tycko, R., Molecular structure of amyloid fibrils: insights from solid-state NMR. *Q. Rev. Biophys.*, 2006, **39**, 1–55.
6. Török, M., Milton, S., Kaye, R., Wu, P., McIntire, T., Glabe, C. G. and Langen, R., Structural and dynamic features of Alzheimer's A β peptide in amyloid fibrils studied by site-directed spin labeling. *J. Biol. Chem.*, 2002, **277**, 40810–40815.
7. Sarkar, N., Kumar, M. and Dubey, V. K., Effect of sodium tetrathionate on amyloid fibril: Insight into the role of disulfide bond in amyloid progression. *Biochimie*, 2011, **93**, 962–968.
8. Hård, T. and Lendel, C., Inhibition of amyloid formation. *J. Mol. Biol.*, 2012, **424**, 441–465.
9. Liu, R., Su, R., Liang, M., Huang, R., Wang, M., Qi, W. and He, Z., Physicochemical strategies for inhibition of amyloid fibril formation: an overview of recent advances. *Curr. Med. Chem.*, 2012, **19**, 4157–4174.
10. Sarkar, N., Kumar, M. and Dubey, V. K., Rottlerin dissolves preformed protein amyloid: a study on hen egg white lysozyme. *BBA-Gen. Subjects*, 2011, **1810**, 809–814.

11. Lannfelt, L. *et al.*, Safety, efficacy, and biomarker findings of PBT2 in targeting $A\beta$ as a modifying therapy for Alzheimer's disease: A phase IIa, double-blind, randomised, placebocontrolled trial. *Lancet Neurol.*, 2008, **7**, 779–786.
12. Yang, F. S. *et al.*, Curcumin inhibits formation of amyloid- β oligomers and fibrils, binds plaques, and reduces amyloid *in vivo*. *J. Biol. Chem.*, 2005, **280**, 5892–5901.
13. Nakagami, Y., Nishimura, S., Murasugi, T., Kaneko, I., Meguro, M., Marumoto, S., Kogen, H., Koyama, K. and Oda, T., A novel β -sheet breaker, RS-0406, reverses amyloid β -induced cytotoxicity and impairment of long-term potentiation *in vitro*. *Br. J. Pharmacol.*, 2002, **137**, 676–682.
14. Porat, Y., Abramowitz, A. and Gazit, E., Inhibition of amyloid fibril formation by polyphenols: Structural similarity and aromatic interactions as a common inhibition mechanism. *Chem. Biol. Drug. Des.*, 2006, **67**, 27–37.
15. Chacon, M. A., Barria, M. I., Soto, C. and Inestrosa, N. C., β -sheet breaker peptide prevents $A\beta$ -induced spatial memory impairments with partial reduction of amyloid deposits. *Mol. Psychiatry.*, 2004, **9**, 953–961.
16. Gordon, D. J., Sciarretta, K. L. and Meredith, S. C., Inhibition of $A\beta_{1-40}$ fibrillogenesis and disassembly of $A\beta_{1-40}$ fibrils by short β -amyloid congeners containing N-methyl amino acids at alternate residues. *Biochemistry*, 2001, **40**, 8237–8245.
17. Grillo-Bosch, D. *et al.*, Retro-enantio N-methylated peptides as-amyloid aggregation inhibitors. *ChemMedChem.*, 2009, **4**, 1488–1494.
18. Granic, I. *et al.*, Leu-Pro-Tyr-Phe-Asp-NH₂ neutralizes $A\beta$ -induced memory impairment and toxicity. *J. Alzheimers Dis.*, 2010, **19**, 991–1005.
19. Kokkoni, N., Stott, K., Amijee, H., Mason, J. M. and Doig, A. J., N-Methylated analogues of β -amyloid aggregation and toxicity: Optimization of the inhibitor structure. *Biochemistry*, 2006, **45**, 9906–9918.
20. Matharu, B., El-Agnaf, O., Razvi, A. and Austen, B. M., Development of retro-inverso peptides as anti-aggregation drugs for β -amyloid in Alzheimer's disease. *Peptides*, 2010, **31**, 1866–1872.
21. Carter, M. D., Simms, G. A. and Weaver, D. F., The development of new therapeutics for Alzheimer's disease. *Clin. Pharmacol. Ther.*, 2010, **88**, 475–486.
22. Fradinger, E. A. *et al.*, C-Terminal peptides co-assemble into $A\beta_{1-42}$ oligomers and protect neurons against $A\beta_{1-42}$ -induced neurotoxicity. *Proc. Natl. Acad. Sci. USA*, 2008, **105**, 14175–14180.
23. Pratim Bose, P. *et al.*, Poly-N-methylated amyloid β -peptide ($A\beta$) C-terminal fragments reduce $A\beta$ toxicity *in vitro* and in *Drosophila melanogaster*. *J. Med. Chem.*, 2009, **52**, 8002–8009.
24. Hilbich, C., Kisters-Woike, B., Reed, J., Masters, C. L. and Beyreuther, K., Substitutions of hydrophobic amino acids reduce the amyloidogenicity of Alzheimer's disease $A\beta$ peptides. *J. Mol. Biol.*, 1992, **228**, 460–473.
25. Jarrett, J. T., Berger, E. P. and Lansbury Jr, P. T., The carboxy terminus of the amyloid protein is critical for the seeding of amyloid formation: Implications for the pathogenesis of Alzheimer's disease? *Biochemistry*, 1993, **32**, 4693–4697.
26. Bansal, S., Maurya, I. K., Yadav, N., Thota, C. K., Kumar, V., Tikoo, K. and Jain, R., C-Terminal fragment, $A\beta_{32-37}$, analogues protect against $A\beta$ aggregation-induced toxicity. *ACS Chem. Neurosci.*, 2016, **7**, 615–623.
27. Kirkwood, J. G., Statistical mechanics of fluid mixtures. *J. Chem. Phys.*, 1935, **3**, 300–313.
28. Torrie, G. M. and Valleau, J. P., Monte Carlo free energy estimates using non-Boltzmann sampling: application to the sub-critical Lennard–Jones fluid. *Chem. Phys. Lett.*, 1974, **28**, 578–581.
29. Crescenzi, O., Tomaselli, S., Guerrini, R., Salvadori, S., D'Ursi, A. M., Temussi, P. A. and Picone, D., Solution structure of the Alzheimer amyloid β -peptide (1–42) in an apolar microenvironment. *Eur. J. Biochem.*, 2002, **22**, 5642–5648.
30. Westbrook, J., Feng, Z., Chen, L., Yang, H. and Berman, H. M., The protein data bank and structural genomics. *Nucleic Acids Res.*, 2003, **31**, 489–491.
31. Jorgensen, W. L., Chandrasekhar, J., Madura, J. D., Impey, R. W. and Klein, M. L., Comparison of simple potential functions for simulating liquid water. *J. Chem. Phys.*, 1983, **79**, 926–935.
32. Case, D. A. *et al.*, AMBER 12, 2012; <http://ambermd.org/doc12/Amber12.pdf>
33. Lindorff-Larsen, K., Piana, S., Palmo, K., Maragakis, P., Klepeis, J. L., Dror, R. O. and Shaw, D. E., Improved side-chain torsion potentials for the Amber ff99SB protein force field. *Proteins: Struct. Funct. Bioinf.*, 2010, **78**, 1950–1958.
34. Berendsen, H. J., Postma, J. V., van Gunsteren, W. F., DiNola, A. R. and Haak, J. R., Molecular dynamics with coupling to an external bath. *J. Chem. Phys.*, 1984, **81**, 3684–3690.
35. Ryckaert, J. P., Ciccotti, G. and Berendsen, H. J., Numerical integration of the cartesian equations of motion of a system with constraints: molecular dynamics of *n*-alkanes. *J. Comput. Phys.*, 1977, **23**, 327–341.
36. Darden, T., York, D. and Pedersen, L., Particle mesh Ewald: An N-log (N) method for Ewald sums in large systems. *J. Chem. Phys.*, 1993, **98**, 10089–10092.
37. DeLano, W. L., The PyMOL Molecular Graphics System, Version 1, DeLano Scientific, Palo Alto, CA, 2002.
38. Guex, N. and Peitsch, M. C., SWISS-MODEL and the Swiss-Pdb Viewer: an environment for comparative protein modeling. *Electrophoresis*, 1997, **18**, 2714–2723.
39. Luhrs, T., Ritter, C., Adrian, M., Loher, B., Bohrmann, D. R., Döbeli, H., Schubert, D. and Riek, R., 3D structure of Alzheimers amyloid- β (1–42) fibrils. *Proc. Natl. Acad. Sci. USA*, 2005, **102**, 17342–17347.
40. Schneidman-Duhovny, D., Inbar, Y., Nussinov, R. and Wolfson, H. J., PatchDock and SymmDock: servers for rigid and symmetric docking. *Nucleic Acids Res.*, 2005, **33**, W363–W367.
41. Kumar, S., Bouzida, D., Swendsen, R. H., Kollman, P. A. and Rosenberg, J. M., The weighted histogram analysis method for free-energy calculations on biomolecules. I. The method. *J. Comput. Chem.*, 1992, **13**, 1011–1021.
42. Humphrey, W., Dalke, A. and Schulten, K., VMD: visual molecular dynamics. *J. Mol. Graph.*, 1996, **14**, 33–38.
43. Sobolev, V., Eyal, E., Gerzon, S., Potapov, V., Babor, M., Prilusky, J. and Edelman, M., SPACE: a suite of tools for protein structure prediction and analysis based on complementarity and environment. *Nucleic Acids Res.*, 2005, **33**, W39–W43.
44. Laskowski, R. A., PDBsum: summaries and analyses of PDB structures. *Nucleic Acids Res.*, 2001, **29**, 221–222.

ACKNOWLEDGEMENTS. We thank Tezpur University for the start-up grant and DBT funded Bioinformatics Infrastructure facility in the Department of Molecular Biology and Biotechnology at Tezpur University.

Received 2 August 2017; revised accepted 20 November 2017

doi: 10.18520/cs/v114/i06/1207-1213